

Decoding Interpretable Logic Rules from Neural Networks

CHUQIN GENG, McGill University, Canada

XIAOJIE XU, McGill University, Canada

ZHAOYUE WANG, McGill University, Canada

ZIYU ZHAO, McGill University, Canada

XUJIE SI, University of Toronto, Canada

As deep neural networks continue to excel across various domains, their black-box nature has raised concerns about transparency and trust. In particular, interpretability has become increasingly essential for applications that demand high safety and knowledge rigor, such as drug discovery, autonomous driving, and genomics. However, progress in understanding even the simplest deep neural networks—such as fully connected networks—has been limited, despite their role as foundational elements in state-of-the-art models like ResNet and Transformer. In this paper, we address this challenge by introducing **NEUROLOGIC**, a novel approach for decoding interpretable logic rules from neural networks. **NEUROLOGIC** leverages neural activation patterns to capture the model’s critical decision-making processes, translating them into logical rules represented by hidden predicates. Thanks to its flexible design in the grounding phase, **NEUROLOGIC** can be adapted to a wide range of neural networks. For simple fully connected neural networks, hidden predicates can be grounded in certain split patterns of original input features to derive decision-tree-like rules. For large, complex vision neural networks, **NEUROLOGIC** grounds hidden predicates into high-level visual concepts that are understandable to humans. Our empirical study demonstrates that **NEUROLOGIC** can extract global and interpretable rules from state-of-the-art models such as ResNet, a task at which existing work struggles. We believe **NEUROLOGIC** can help pave the way for understanding the black-box nature of neural networks.

CCS Concepts: • **Do Not Use This Code** → **Generate the Correct Terms for Your Paper**; *Generate the Correct Terms for Your Paper*; *Generate the Correct Terms for Your Paper*; *Generate the Correct Terms for Your Paper*.

1 Introduction

In recent years, deep neural networks (DNNs) have made remarkable progress across various domains, including computer vision [He et al. 2016; Krizhevsky et al. 2012], speech recognition [Hinton et al. 2012], and natural language processing [Sutskever et al. 2014], among others [Silver et al. 2017]. Products powered by DNN-based systems, such as large language models (LLMs) [Zhao et al. 2023], have become integral to daily life and are now utilized by billions of people. Their significance is anticipated to grow even further in the foreseeable future. Despite their impressive performance, the black-box nature of DNNs poses significant challenges in understanding their internal workings. Empirical studies indicate that the mechanisms underlying DNNs may differ fundamentally from human cognition, leading to unpredictable behaviors [Szegegy et al. 2014].

Meanwhile, the need for interpretability in DNNs has become crucial, as highlighted in several cases [Doshi-Velez and Kim 2017; Guidotti et al. 2018; Lipton 2016]: First, interpretability is essential for prediction systems that require high reliability, where unexpected errors could lead to catastrophic outcomes, such as loss of life or substantial financial damage. It enables domain experts to detect potential issues early and helps engineers identify root causes, facilitating effective problem-solving. Second, interpretability is critical in applications where fairness and accountability are important, such as in healthcare, finance, and legal domains. For example, DNNs are increasingly employed in drug discovery and design [Gawehn et al. 2016], where regulatory bodies like the FDA

Authors’ Contact Information: Chuqin Geng, chuqin.geng@mail.mcgill.ca, McGill University, Canada; Xiaojie Xu, xiaojie.xu@mail.mcgill.ca, McGill University, Canada; Zhaoyue Wang, zhaoyue.wang@mail.mcgill.ca, McGill University, Canada; Ziyu Zhao, ziyu.zhao2@mail.mcgill.ca, McGill University, Canada; Xujie Si, six@cs.toronto.edu, University of Toronto, Canada.

mandate that models be interpretable to understand the biological mechanisms underlying clinical results. Third, DNNs serve as powerful tools in research fields that involve complex data patterns, such as genomics [Park and Kellis 2015], astronomy [Parks et al. 2018], physics [Baldi et al. 2014], and social science [Hofman et al. 2017]. By enhancing interpretability, we can uncover hidden insights and knowledge captured by these models, transforming them into scientific discoveries.

Existing research in the interpretability of neural networks can be categorized based on explanatory power [Zhang et al. 2021a], ranging from prototypes, attributions, and hidden semantics to logic rules, in increasing order. For instance, Grad-CAM [Selvaraju et al. 2017] is an attribution method, while Network Dissection [Bau et al. 2017] is a hidden semantics method. Among these, methods that produce global logic rules over sets of inputs, as opposed to local rules applied to individual samples, are recognized as providing stronger interpretability and are highly preferred [Pedreschi et al. 2019], which is also the focus of this paper. Earlier work on logic extraction from neural networks dates back to the pre-deep learning era of the 1990s [Fu 1991; Setiono and Liu 1995, 1997; Towell and Shavlik 1993], and was therefore developed for relatively small datasets, such as the Iris dataset. These approaches primarily adapt search techniques for combinations of specific value ranges in input attributes, cluster the activation values of hidden neurons, and perform layer-by-layer rule generation and rewriting. However, these methods tend to produce single decision tree-like rules, which often lead to an unfaithful approximation of the underlying neural network. They also face scalability challenges, making them especially unsuitable as neural networks become deeper in modern applications. As a result, more recent "rule as explanation" methods shift toward local interpretability on individual samples [Wang 2019; Wu et al. 2020].

To this end, our proposed method, NEUROLOGIC, aims to provide a modern logic rule-based approach with global interpretability suited for the era of deep learning. NEUROLOGIC can be decomposed into three phases: *distilling*, *decoding*, and *grounding*. Firstly, in the *distilling* phase, we leverage neural activation patterns (NAPs) [Geng et al. 2023, 2024]—a subset of neurons that exhibit similar behavior for inputs belonging to the same class—to distill the critical reasoning processes of neural networks. Specifically, for a chosen layer, we identify a set of class-specific neurons from the NAP at that layer, which are responsible for classification decisions for the corresponding classes.

Secondly, in the *decoding* phase, we identify a set of salient neurons in the preceding layer, with a focus on those that contribute most significantly to the class-specific neurons, as measured by the average of $w_i x_i$. These salient neurons are expected to capture the model’s crucial decision-making processes for the respective class, exhibiting notably higher activation values compared to those of other classes. We then determine the optimal threshold within the activation ranges for each salient neuron, converting them into hidden predicates. These predicates encode high-level representations of input features, with a true value assignment to a predicate indicating the presence of the associated representation for a given input. Finally, NEUROLOGIC generates a set of logic rules based on these hidden predicates in a data-driven manner.

Thirdly, in the *grounding* phase, NEUROLOGIC aims to ground hidden predicates to the original input space. In fully connected neural networks, these hidden predicates act as linear constraints on input features, defining decision regions where the logic rules correspond to unions of convex regions that approximate the data manifold. To further enhance interpretability, domain knowledge can be utilized to translate these linear constraints into a form more understandable to humans. Additionally, if the data can be reasonably assumed to follow bounding box priors—that is, if it can be represented by splits on individual features, the decision boundaries of the linear predicates can be refined to resemble a decision-tree-like structure. We demonstrate that this refinement problem can be formulated as a Mixed-Integer Linear Program (MILP) and validate its effectiveness with a case study. In the context of large, complex classification neural networks, such as ResNet, NEUROLOGIC operates on the output layer, where the resulting predicates have decision regions

that are difficult to describe, as the inputs must undergo a series of complex transformations to reach them. To this end, we propose a causal inference approach to interactively identify regions of interest in the input space, where the absence of these regions can cause a predicate to be evaluated as False. Then we feed those regions collected from a set of inputs to human agent to recognize the high-level concepts that presented among those regions. In this way, we are able to reveal the hidden reasoning processes of state-of-the-art vision models like ResNet. For instance, we extract a logical rule showing that ResNet classifies an image as a dog based on the presence of visual parts such as the "nose", "legs", and "ears". To the best of our knowledge, this is the first time a complex CNN has been interpreted through explicit logical rules, represented by human-understandable visual concepts. In contrast, existing work [Jiang et al. 2024] only observes rule-like structures, such as "compositional" behavior in CNNs. Our contributions can be summarized as follows:

- We present a novel framework, NEUROLOGIC, for extracting global and interpretable rules from neural networks. NEUROLOGIC also remains faithful to the decision-making process of the original model, thereby helping to unravel the black-box nature of neural networks.
- We demonstrate that the reasoning processes of neural networks can be approximated and extracted using neural activation patterns, combined with identifying salient neurons and learning optimal thresholds. This approach yields a first-order logic (FOL) representation with hidden predicates.
- We introduce new ideas and algorithms for grounding hidden predicates in the input space. For fully connected networks, we discuss three types of explanations: linear constraints, domain knowledge, and bounding boxes. For large, complex neural networks, we show how predicates can be grounded in human-understandable concepts via causal inference.
- We empirically evaluate NEUROLOGIC on challenging instances, including state-of-the-art vision models like ResNet, demonstrating its capacity to extract global and interpretable rules from neural networks, a task at which existing work struggles.

2 Background

In this section, we introduce foundational concepts and notation for fully connected neural networks in classification tasks, along with the neural activation pattern (NAP) and first-order logic.

2.1 Neural Networks for Classification Tasks

In this paper, we focus on fully connected neural networks (FCNs) using the ReLU activation function. Generally speaking, a feed-forward network N consists of L layers, each performing a linear transformation followed by ReLU activation. For the l -th layer, we define the pre-activation and post-activation values as $z^{(l)}(x)$ and $\hat{z}^{(l)}(x)$, respectively. The computation is given by:

$$z^{(l)}(x) = \mathbf{W}^{(l)}\hat{z}^{(l-1)}(x) + \mathbf{b}^{(l)}, \quad \hat{z}^{(l)}(x) = \text{ReLU}(z^{(l)}(x)),$$

where $\mathbf{W}^{(l)}$ and $\mathbf{b}^{(l)}$ are the weight matrix and bias of the layer. Each layer l has d_l neurons, with $N_{i,l}$ representing the i -th neuron in that layer. For an input x , the pre-activation and post-activation values of $N_{i,l}$ are $z_i^{(l)}(x)$ and $\hat{z}_i^{(l)}(x)$, respectively. The network as a whole functions as $\mathbf{F}^{<N>} : \mathbb{R}^{d_0} \rightarrow \mathbb{R}^{d_L}$, mapping input x to the final layer output $z^{(L)}(x)$, with $\mathbf{F}_i^{<N>}(x) := z_i^{(L)}(x)$ for the i -th output neuron. For simplicity, we will omit N when contextually clear. In a multi-class classification setting, given an input x and class set C , the network assigns x to class $c \in C$ if $\mathbf{F}_c(x)$, the c -th neuron output in layer L , is the maximum among all classes.

In many complex neural network architectures such as ResNet and Transformers, a simple fully connect layer is commonly used as the final classification head. Thus, they can be represented as a

simple FCN:

$$\mathbf{F}(x) = \mathbf{W}^{(L)} z^{(L-1)}(x) + \mathbf{b}^{(L)}$$

where $z^{(L-1)}(x)$ are hidden representations learned at layer $L - 1$. The resulting output, $\mathbf{F}(x)$, provides the final classification logits, with each class score $\mathbf{F}_c(x)$ being derived from a weighted sum of the post-activation values from the preceding layer.

2.2 Neural Activation Patterns

Neuron State Abstractions. To better characterize an individual neuron’s behavior, we define abstractions on neurons. Specifically, for an internal neuron $N_{i,l}$ (where $0 \leq i \leq d_l$ and $1 \leq l \leq L-1$) in the neural network N , its post-activation value $\hat{z}_i^{(l)}(x)$ can be abstracted into finite states. A simple binary abstraction for ReLU activation defines two states: $\mathbf{0}$ (deactivation), representing a value of 0, and $\mathbf{1}$ (activation), representing values in the range $(0, \infty)$. Furthermore, these states can be abstracted into a coarser state $*$ $= [0, \infty)$, covering the entire range of post-activation values. This leads to a partial order: $* \leq \mathbf{0}$ and $* \leq \mathbf{1}$, where $\mathbf{0}$ and $\mathbf{1}$ refine $*$. Intuitively, being in the state $*$ implies that the neuron can be either in the state $\mathbf{0}$ or $\mathbf{1}$.

Definition 2.1 (Neural Activation Pattern). Given a neural network N , we denote the neuron state abstraction of an internal neuron $N_{i,l}$ as $\mathcal{P}_{i,l}$. A neural activation pattern (NAP) \mathcal{P} is defined as a tuple that captures the abstraction states of all neurons within the network N . Formally, it is expressed as:

$$\mathcal{P} := \langle \mathcal{P}_{i,l} \mid N_{i,l} \in N \rangle,$$

where each $\mathcal{P}_{i,l}$ can take one of the abstraction states $*$, $\mathbf{0}$, or $\mathbf{1}$. Consequently, the Neural Activation Pattern (NAP) captures the overall behavior of the neural network by providing a summary of the activation states of its individual neurons.

Local NAP Induced by a Single Input x . The previously defined NAP serves as a general conceptual tool but does not provide specific guidance on how to compute the NAP in practice. Therefore, we define \mathcal{P}^x , the local NAP induced by a single input x . Specifically, when an input x is passed through an internal neuron $N_{i,l}$, the corresponding abstraction state $\mathcal{P}_{i,l}^x$ can be determined based on its post-activation value $\hat{z}_i^{(l)}(x)$:

$$\mathcal{P}_{i,l}^x = \mathbf{0} \text{ if } \hat{z}_i^{(l)}(x) = 0; \quad \mathcal{P}_{i,l}^x = \mathbf{1} \text{ if } \hat{z}_i^{(l)}(x) > 0$$

\mathcal{P}^x records the decision-making path of the neural network N when making a prediction on x .

Global NAP Induced by a Set of Inputs X . \mathcal{P}^x is considered local as it helps explain the network’s predictions for individual samples. To gain general insights into how N makes decisions for a set of inputs X , specifically X_c (where X_c contains inputs belonging to a certain class $c \in C$), we need to compute a global NAP, denoted as \mathcal{P}^X or \mathcal{P}^c . However, a challenge arises when two distinct inputs may lead to conflicting abstraction states for a neuron; for instance, a neuron may be deactivated for input x_1 (i.e., $\mathcal{P}_{i,l}^{x_1} = \mathbf{0}$) but activated for another input x_2 (i.e., $\mathcal{P}_{i,l}^{x_2} = \mathbf{1}$). In such situations, we can coarsen the neuron’s state to $*$, resulting in $\mathcal{P}_{i,l}^{\{x_1, x_2\}} = *$. However, to prevent all neurons from being abstracted into $*$, we introduce the parameter δ to allow inputs to vote on a neuron’s state, as suggested in previous work [Geng et al. 2023, 2024]. Formally, this can be described as:

$$\mathcal{P}_{i,l}^X = \begin{cases} \mathbf{0} & \text{if } \frac{|\{x_j \mid \mathcal{P}_{i,l}^{x_j} = \mathbf{0}, x_j \in X\}|}{|X|} \geq \delta \\ \mathbf{1} & \text{if } \frac{|\{x_j \mid \mathcal{P}_{i,l}^{x_j} = \mathbf{1}, x_j \in X\}|}{|X|} \geq \delta \\ * & \text{otherwise} \end{cases} \quad (1)$$

For example, if δ is set to 0.95, the neuron will be in the **1** state only if 95% or more of the inputs indicate activation. This is crucial for mining meaningful global NAPs in standard classification settings, where Type I and Type II errors are non-negligible.

Definition 2.2 (Global NAPs Subsuming Local NAPs). We say that a global NAP \mathcal{P}^X subsumes a local NAP \mathcal{P}^x if, for each neuron $N_{i,l}$, the state in \mathcal{P}^X is an abstraction of its state in \mathcal{P}^x . Formally, this relationship is defined as:

$$\mathcal{P}^X \leq \mathcal{P}^x \iff \mathcal{P}_{i,l}^X \leq \mathcal{P}_{i,l}^x \quad \forall N_{i,l} \in N.$$

Additionally, we say an input x follows a global NAP \mathcal{P}^X if its local NAP is subsumed by \mathcal{P}^X .

To better illustrate the above definitions and notations, we consider a simple 2x2 fully connected neural network with neurons $N_{0,1}, N_{1,1}, N_{0,2}, N_{1,2}$ as an example. Suppose we have two instances, x_1 and x_2 , with local NAPs $\langle \mathbf{1}, \mathbf{0}, \mathbf{1}, \mathbf{0} \rangle$ and $\langle \mathbf{1}, \mathbf{1}, \mathbf{1}, \mathbf{0} \rangle$, respectively. We can then compute a global NAP $\langle \mathbf{1}, *, \mathbf{1}, \mathbf{0} \rangle$, which both x_1 and x_2 follow, i.e., $\langle \mathbf{1}, *, \mathbf{1}, \mathbf{0} \rangle \leq \langle \mathbf{1}, \mathbf{0}, \mathbf{1}, \mathbf{0} \rangle$ and $\langle \mathbf{1}, *, \mathbf{1}, \mathbf{0} \rangle \leq \langle \mathbf{1}, \mathbf{1}, \mathbf{1}, \mathbf{0} \rangle$. However, for x_3 with a local NAP of $\langle \mathbf{0}, \mathbf{0}, \mathbf{1}, \mathbf{0} \rangle$, it does not follow this global NAP.

2.3 First-Order Logic

Logic rules are highly interpretable to humans and have a long history of research, making rule extraction a promising method for understanding neural networks. Typically, rule extraction techniques aim to provide *global* explanations by deriving a single set of rules from the target model. A fundamental rule structure can be expressed as:

$$\text{If } P, \text{ then } Q$$

where P serves as the antecedent and Q as the consequent. In the context of interpreting the rules encoded by neural networks, Q represents the network's prediction (e.g., a class label), while the antecedent P generally combines multiple conditions related to the input features. In complex models, explanatory rules can take various forms, including propositional, first-order, or fuzzy rules. In this work, we primarily focus on first-order rules.

First-Order Logic (FOL), also referred to as Predicate Logic, is a formal system utilized in various fields such as mathematics, philosophy, linguistics, and computer science. FOL extends propositional logic by incorporating quantifiers, variables, and predicates, which enable more expressive statements about objects and their properties. The key components of FOL include:

- **Constants:** They represent specific objects or individuals in the domain, such as a , $john$, and 3 .
- **Variables:** They symbolize arbitrary objects in the domain, typically denoted as x , y , z , and can be quantified, e.g., "for all x " or "there exists an x ".
- **Predicates:** They are functions that express relationships or properties of objects, taking one or more arguments and returning a truth value. For instance, $Loves(x, y)$ might indicate "x loves y," while $P(x)$ could mean "x is a person."
- **Quantifiers:** They facilitate generalization over objects. The *universal quantifier* (\forall) signifies "for all," exemplified by $\forall x P(x)$, i.e., " $P(x)$ is true for all x ". The *existential quantifier* (\exists) denotes "there exists," as shown in $\exists x P(x)$, i.e., "There exists an x such that $P(x)$ is true".
- **Logical Connectives:** These include *AND* (\wedge), *OR* (\vee), *NOT* (\neg), *Implies* (\implies), and *If and Only If* (\iff), which are used to combine predicates into complex statements.
- **Functions:** They represent operations on objects that return a single object, such as $father(x)$. Constants are 0-ary functions.

The syntax of FOL includes both atomic and complex formulas. An atomic formula is a predicate applied to one or more terms (constants, variables, or functions), such as $P(x)$ or $Loves(john, mary)$.

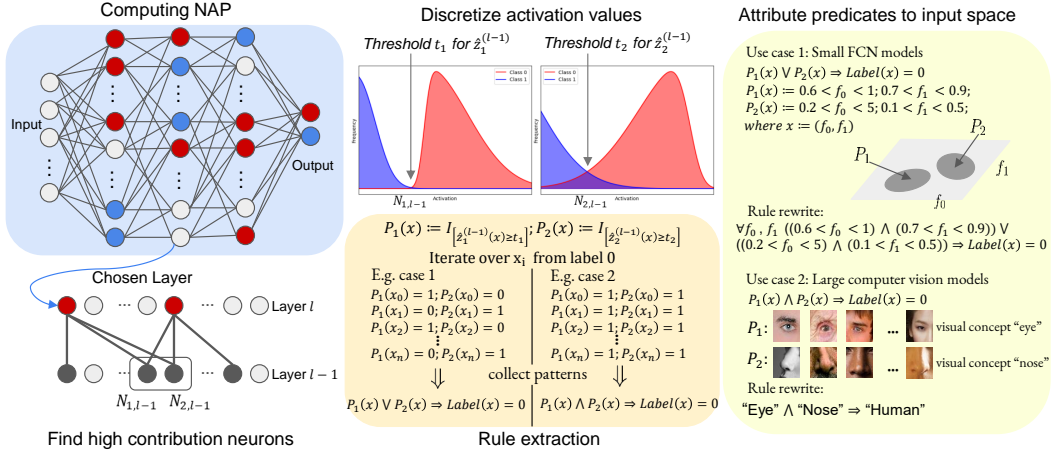


Fig. 1. Overview of the NEUROLOGIC Framework.

A complex formula is created by combining atomic formulas with logical connectives and quantifiers. For example, a possible FOL statement extracted from a classification model could be: if all inputs satisfy $P_1(x) \wedge P_2(x) \wedge P_3(x)$, or if $P_4(x)$ holds, they will be labeled as class 1:

$$\forall x (P_1(x) \wedge P_2(x) \wedge P_3(x)) \vee P_4(x) \Rightarrow Label(x) = 1$$

Additionally, the semantics of FOL are interpreted in terms of a domain of discourse, which is the set of objects that the variables can reference. An interpretation assigns meanings to constants, predicates, and functions, determining the truth value of a formula based on the truth of the predicates for specific objects.

3 The NEUROLOGIC Framework

In this section, we introduce NEUROLOGIC, a novel approach for decoding interpretable logic rules from neural networks, and provide a detailed discussion of our proposed methodology and design choices. We begin with an overview of the NEUROLOGIC framework.

3.1 Overview

Neural networks are typically viewed as 'black boxes,' making it challenging to interpret how they arrive at particular classification decisions. NEUROLOGIC aims to address this challenge by providing an effective method for translating the network's learned internal patterns into interpretable logic rules through a series of steps, as illustrated in Figure 1.

The process begins with computing the neural activation pattern of the neural network across different layers for each class. Next, within a chosen layer of the NAPs, we select a set of class-specific neurons responsible for encoding hidden representations of the corresponding class. The framework then identifies a set of important neurons in the previous layer, focusing on those that contribute most significantly to these class-specific neurons. The activation ranges of these high-contribution neurons are then discretized using learned thresholds, yielding a collection of predicates relevant to each class. NEUROLOGIC then extracts logical rules that describe the relationship between these predicates and the class labels in a data-driven manner. Initially, these extracted rules are expressed in terms of predicates that capture much of the model's decision-making. The predicates are then grounded in the input feature space. Finally, by combining logic rules derived from the hidden layers with the rules describing the grounding of predicates in input features—or human-understandable

concepts manifested in the input space—NEUROLOGIC generates a final set of logical rules that accurately describe the network’s behavior in an interpretable and input-grounded form.

Algorithm 1 outlines the high-level procedure of the NEUROLOGIC framework. It takes as input a neural network (N), a dataset (X), and a chosen layer (l), typically the second hidden layer or the final output layer, and returns a set of FOL rules \mathcal{R} . For ease of discussion, we divide the NEUROLOGIC framework into three phases: *distilling*, *decoding*, and *grounding*, with each phase integrating relevant procedures to achieve its intended purpose.

Algorithm 1: NEUROLOGIC: Logic Rule Extraction from Neural Networks

Input: Neural Network (N), Dataset (X), Chosen Layer (l)

Output: A set of FOL rules \mathcal{R}

```

1 Function NeuroLogic( $N, X, l$ )
2    $A \leftarrow \text{ComputeActivations}(N, X)$            /* Compute activations for all inputs in  $X$  */
3   for  $c \in \text{Classes}$  do
4      $X_c, A_c \leftarrow \text{FilterClass}(X, A, c)$        /* Filter inputs, activations for class  $c$  */
5      $\mathcal{P}_c \leftarrow \text{ComputeActivationPatterns}(A, X_c)$ 
6      $\Omega \leftarrow \text{SelectLayerNeurons}(\mathcal{P}_c, l)$      /* Get NAP slice at layer  $l$  */
7      $\Theta \leftarrow \text{SelectSalientNeurons}(\Omega, l - 1)$  /* Identify key neurons at layer  $l - 1$  */
8      $T \leftarrow \text{DiscretizeActivations}(\Theta, A)$    /* Determine activation ranges */
9      $\mathcal{R}_c^H \leftarrow \text{ExtractRules}(\Theta, T, A_c)$    /* Extract rules on hidden-layer predicates */
10     $\mathcal{R}_c^I \leftarrow \text{GroundToInputFeatures}(\Theta, X_c)$  /* Attribute predicates to input space */
11     $\mathcal{R}_c \leftarrow \text{ConstructFinalRules}(\mathcal{R}_c^H, \mathcal{R}_c^I)$  /* Combine hidden and input rules */
12   $\mathcal{R} \leftarrow \{\mathcal{R}_c \mid c \in \text{Classes}\}$ 
13  return  $\mathcal{R}$ 

```

3.2 Distilling Phase: Identifying the Critical Decision-Making Processes of Neural Networks via Neural Activation Patterns

Neural networks are known to exhibit highly sparse structures [Liang et al. 2021], with recent studies indicating that removing even over 95% of neurons causes only a 1.83% drop in accuracy on ResNet-50 when evaluated on the ImageNet benchmark [Georgoulakis et al. 2023]. In the spirit of Occam’s Razor, eliminating redundant structures, such as neuron connections, is crucial for understanding how a model works. This insight suggests that neural networks can be faithfully approximated using a much smaller subnetwork, which has led to the common adoption of pruning or distillation techniques in existing work on rule extraction from neural networks [Setiono and Liu 1995, 1997]. However, these pruning-based methods often overlook class-specific differences in the models’ reasoning mechanisms. They typically perform pruning based on the magnitude of weights, under the assumption that the resulting pruned network can serve as a universal decision-making process for all classes. We argue that this assumption is overly simplistic. In reality, each class possesses its own unique decision-making process [Geng et al. 2023]. Therefore, in our approach, we focus on distilling the decision-making process for each class individually, using neural activation patterns (NAPs) as a more accurate approximation of neural network behavior. We refer to this approach as distillation, as it aims to extract class-specific information, distinguishing it from traditional pruning methods.

We start by computing the global NAP \mathcal{P}^c for each class $c \in C$ based on Equation 1. Intuitively, each local NAP \mathcal{P}^x captures the decision-making process made by the model N for an individual input x , through the abstraction of the activation values for each $x \in X_c$. To gain a unified view on X_c , all the inputs from the class c , we compute \mathcal{P}^c , which reflects the critical decision paths for

class c . Next, given a chosen layer l – typically the second hidden layer or the final output layer – we select a set of activated neurons Ω from the slice of global NAPs at layer l . These neurons are class-specific and are not shared between classes. In this sense, Ω , which exclusively represents class c at layer l , acts as a proxy for the output neurons corresponding to class c in the final layer. This allows us to use the first l layers to approximate the behavior of the full neural network N . Thus, the remaining task is to decode logic rules from this l -layer subnetwork.

Algorithm 2: Identification of high-contribution neurons for the class c at layer $l - 1$

Input: Neural Network (N), Dataset (X_c), Class-specific neurons (Ω), Chosen layer (l), Parameter (k)

Output: Set of high-contribution neurons Θ

```

1 Function SelectSalientNeurons( $N, \Omega, X_c, l, k$ )
2   for  $j \in \Omega$  do
3     for  $i \in N_{l-1}$  do
4        $c_{ij} \leftarrow \frac{1}{|X_c|} \sum_{x \in X_c} \mathbf{W}_{ji}^{(l)} \hat{z}_i^{(l-1)}(x)$  /* Compute the mean contribution of  $i$  to  $j$  */
5        $C_j \leftarrow \{c_{ij} \mid i \in N_{l-1}\}$  /* Contribution vector for class-specific neuron  $j$  */
6       sort  $C_j$  in descending order /* Sort by contribution */
7        $\Theta^j \leftarrow \text{TopK}(C_j, k)$  /* Select top  $k$  neurons */
8    $\Theta \leftarrow \bigcup_{j \in \Omega} \Theta^j$  /* Union of top neurons across */
9   return  $\Theta$ 

```

3.3 Decoding Phase: Translating the Neural Network Decision-Making Process into FOL Rules with Interpretable Predicates

In this phase, our objective is to construct logic rules using predicates from layer $l - 1$ to explain the class-specific neurons at layer l . To accomplish this, we first identify a set of neurons at layer $l - 1$ that significantly contribute to the computation of class-specific neurons, denoted as Θ . Recall that the activation value of a specific class-specific neuron at layer l , denoted as $\hat{z}_j^{(l)}(x)$, is computed as the sum of the weighted activations from the previous layer:

$$\hat{z}_j^{(l)}(x) = \text{ReLU}(z_j^{(l)}(x)), \quad z_j^{(l)}(x) = \sum_i \mathbf{W}_{ji}^{(l)} \hat{z}_i^{(l-1)}(x) + \mathbf{b}_j^{(l)}.$$

We then sort all the neurons $N_{i,l-1}$ in layer $l - 1$ based on their average contribution to $\hat{z}_j^{(l)}(x)$, given by $\mathbf{W}_{ji}^{(l)} \hat{z}_i^{(l-1)}(x)$, across the entire dataset for label c . Finally, we select the top k neurons for each class-specific neuron. By taking the union of these selected neurons, we obtain Θ , as summarized in Algorithm 2. Notably, our empirical results show that these high-contribution neurons are often shared across multiple class-specific neurons in Ω . Such overlapping high-contribution neurons likely represent foundational patterns learned by the network, allowing it to generalize well to unseen data while maintaining discriminative power for class-specific details.

For each neuron in Θ , inputs from class c generally exhibit significantly higher activation values compared to those from other classes. This is because these neurons serve as latent representations or features specific to class c at layer $l - 1$, as observed by [Geng et al. 2024]. To leverage this, we aim to establish a threshold t for each neuron in Θ that discriminates between inputs from class c and those from other classes based on their activation values. Specifically, if $\hat{z}_j^{(l-1)}(x) \geq t$, the input x should be classified as belonging to class c ; otherwise, it should be classified as belonging to another class. However, setting this threshold poses a challenge: if the threshold is too low, false positives may increase, as many inputs from other classes could be misclassified as class c . Conversely, setting the threshold too high could lead to false negatives, where inputs from class c are incorrectly excluded. To this end, we measure the goodness of a certain threshold t using the

purity metric, defined as:

$$\text{Purity}(t) = \frac{|\{x \in X_c : \hat{z}_j^{(l-1)}(x) \geq t\}|}{|X_c|} + \frac{|\{x \in X_{-c} : \hat{z}_j^{(l-1)}(x) < t\}|}{|X_{-c}|}$$

where X_{-c} represents the set of inputs from classes other than c . A high purity value indicates that most data points are correctly classified into their respective classes, while a low purity value suggests that the classification is less accurate and the data points are more mixed.

To find the optimal threshold t , we perform a linear search across evenly spaced values within the range from 0 to the mean activation value for class c . The goal is to identify the threshold that maximizes purity, as summarized in Algorithm 3.

Algorithm 3: Determine activation ranges for high-contribution neurons

Input: Activation values (A), High-contribution neurons (Θ), Number of steps (m)

Output: The collection of optimal thresholds T

```

1 Function DiscretizeActivations( $A, \Theta, m$ )
2   for  $j \in \Theta$  do
3      $best\_t_j \leftarrow 0, best\_p_j \leftarrow -\infty, step \leftarrow \frac{mean(A_c)}{m}$ 
4     for  $i \leftarrow 0$  to  $m - 1$  do
5        $t_j \leftarrow i \cdot step$ 
6        $purity \leftarrow ComputePurity(t_j, A, \Theta_j)$ 
7       if  $purity > best\_p_j$  then
8          $best\_p_j \leftarrow purity$ 
9          $best\_t_j \leftarrow t_j$ 
10     $T \leftarrow \{best\_t_j | j \in \Theta\}$ 
11  return  $T$ 

```

We then construct a set of predicates P_j at layer $l - 1$ for each neuron in Θ , along with the corresponding threshold t_j , defined as $P_j(x) := \mathbb{I}_{\hat{z}_j^{(l-1)}(x) \geq t_j}$. In this context, a True assignment indicates the presence of the specific latent feature of class c for input x , while a False assignment signifies its absence. Clearly, if an input x activates more predicates as True, it suggests a stronger association with the corresponding class c . However, this raises the question: to what extent should we believe that x belongs to class c based on the pattern of predicate activations?

We address this question using a data-driven approach. Specifically, we feed all inputs from class c to those predicates and collect their corresponding activation patterns¹. For instance, suppose we have four predicates $P_1(x), P_2(x), P_3(x), P_4(x)$ (we will omit x when the context is clear), and five distinct inputs yield the following patterns: (1, 1, 1, 1), (1, 1, 1, 0), (1, 1, 1, 0), (1, 1, 0, 1), and (1, 1, 0, 1). We can then create a disjunction of the distinct conjunctive forms to derive a rule:

$$\forall x \quad (P_1 \wedge P_2 \wedge P_3 \wedge P_4) \vee (P_1 \wedge P_2 \wedge P_3 \wedge \neg P_4) \vee (P_1 \wedge P_2 \wedge \neg P_3 \wedge P_4) \Rightarrow Label(x) = c.$$

In practice, neural networks trained for classification tasks function as discriminators rather than generative models. This suggests that not every class will have a specific reasoning path characterized by the activation of a certain set of hidden features or predicates. Instead, classes can be represented by the deactivation of predicates associated with other classes, as long as the inference remains clear and unambiguous. This highlights the efficient internal encoding of neural networks, which serves as important priors for models aiming to achieve sound classification

¹In this work, we use conjunctive forms and predicate activation patterns interchangeably.

results [Bengio et al. 2013]. It is interesting to note that NEUROLOGIC can even faithfully mirror such phenomena in neural networks, as we will discuss in a case study in Section 4.

3.4 Grounding Phase: Attributing Predicates to the Input Feature Space

Previous research defines interpretability as the ability to provide explanations in understandable terms to a human [Doshi-Velez and Kim 2017]. Ideally, these explanations take the form of logical decision rules, using understandable terms that are grounded in domain knowledge relevant to the task. In our decoding phase, we successfully obtain logical rules with hidden predicates as our explanations. Then the next step is to ground these hidden predicates to terms that are understandable to humans. However, this presents a challenge: there is no universal solution, as what constitutes ‘understandable terms’ or ‘domain knowledge’ is subjective. This issue becomes especially pronounced as deep learning models process increasingly complex data, such as images, making it more difficult for people to interpret the model based on its original input features.

To address this, we design NEUROLOGIC in a decoupled manner, ensuring the grounding phase remains flexible and adaptable to various tasks and models. To facilitate this design, NEUROLOGIC offers flexibility in operating on different layers, adapting to a wide range of classification models. For fully connected networks, it typically operates on the second hidden layer, while for large, complex neural networks with a single fully connected output layer, such as image classification models, it operates on the output layer. We further outline general frameworks for grounding predicates in these two categories.

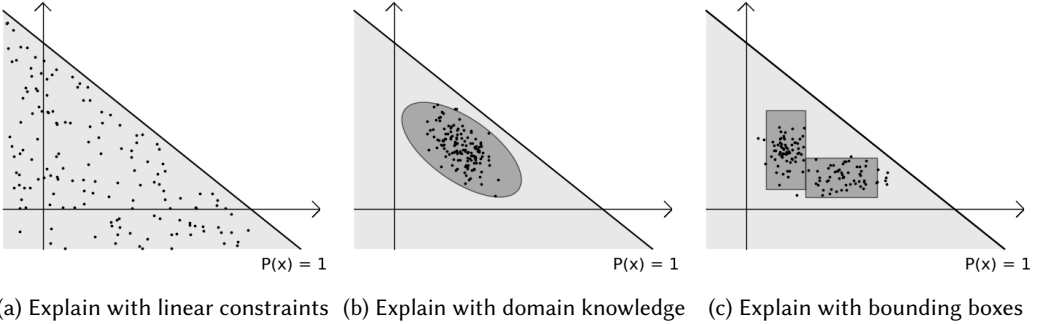


Fig. 2. Three types of explanations of predicates in the input feature space.

Grounding predicates in fully connected networks. For relatively simple fully connected neural networks, such as those trained on the Iris dataset, NEUROLOGIC operates on the second hidden layer. Consequently, each predicate (from the first hidden layer) is represented as a linear half-plane in the high-dimensional input space. In this context, we refer to these predicates as linear. Formally, each linear predicate can be expressed as:

$$P_j(x) = \mathcal{I}_{\hat{z}_j^{(1)}(x) \geq t_j} = \mathcal{I}_{\mathbf{W}_j^{(1)}x + \mathbf{b}_j^{(1)} \geq t_j}, \quad P_j(x) \text{ is true} \Leftrightarrow x \in \{x \mid \mathbf{W}_j^{(1)}x + \mathbf{b}_j^{(1)} \geq t_j\}$$

The linear half-planes defined by each predicate collectively form the decision region of rule models extracted by NEUROLOGIC. This observation aligns with recent studies on the linear regions of neural networks [Geng et al. 2022; Hanin and Rolnick 2019a,b], where linear regions act as learning priors for the network. Unlike the rectangular-like regions employed by decision trees, as shown in Figure 2c, neural networks, along with our extracted rule model, have much greater flexibility in approximating complex decision boundaries using linear half-planes. However, linear boundaries

may not always capture the essence of the data manifold, as data can exhibit certain patterns that are easier for humans to understand. To address this, we categorize three types of explanations for predicates in the input feature space:

- (1) *Explain predicates directly with linear constraints.* In scenarios where the data do not exhibit a specific pattern but are governed by linear predicates, as illustrated in Figure 2a, linear constraints on input features provide the most straightforward explanation. This can be useful in cases where we want to learn unknown constraints of the underlying problem.
- (2) *Explain with domain knowledge.* By leveraging domain knowledge, the decision regions that predicates attempt to approximate can be interpreted in complex, yet comprehensible forms. For example, a group of data forming a shape like an ellipse, as shown in Figure 2b, may be interpreted as a high-dimensional Gaussian distribution.
- (3) *Explain with bounding boxes.* By assuming that data follow bounding box priors, as illustrated in Figure 2c, we can refine the decision boundaries of linear predicates, representing them as splits on individual features, i.e., in the fashion of decision trees. Such explanations are easier for human to understand, especially in low-dimensional spaces.

Bounding boxes or rectangles are among the simplest shapes used to approximate complex decision boundaries defined by linear predicates. Here, we present a general problem formulation as a Mixed-Integer Linear Program (MILP) to solve for these approximate bounding boxes.

We first define m bounding boxes, each characterized by lower and upper bounds for each dimension, represented by vectors $\mathbf{x}_{\min,k}$ and $\mathbf{x}_{\max,k}$, where $1 \leq k \leq m$. We initialize the bounds with the extreme values of the corresponding features, so the bounding boxes can be 'open,' similar to the rules produced by decision trees. The objective is to maximize the number of data points contained within these boxes. A binary decision variable $\alpha_{i,k}$ indicates whether point i is inside bounding box k . With n d -dimensional data points, the objective is to maximize the total number of points within the bounding boxes, expressed as:

$$\text{Maximize} \quad \sum_{i=1}^n \sum_{k=1}^m \alpha_{i,k}$$

subject to:

$$x_{\min,k,j} \leq x_{ij} + M(1 - \alpha_{i,k}), \quad \forall i, j, k$$

$$x_{ij} \leq x_{\max,k,j} + M(1 - \alpha_{i,k}), \quad \forall i, j, k$$

$$\sum_{k=1}^m \alpha_{i,k} \leq 1, \quad \forall i$$

$$\alpha_{i,k} \in \{0, 1\}, \quad \forall i, k$$

$$W\mathbf{x}_{\text{corner},k}^{(\lambda)} \leq T - b, \quad \forall \lambda = 1, \dots, 2^d, \quad \forall k$$

where $1 \leq j \leq d$, and M is a large constant used to relax the constraint when $\alpha_{i,k} = 0$; $\sum_{k=1}^m \alpha_{i,k} \leq 1$ ensures that each data point can only be contained in one bounding box (Non-Overlapping Constraints); and $W\mathbf{x}_{\text{corner},k}^{(\lambda)} \leq T - b$ represents the linear constraints imposed by predicates on the corner points of the bounding boxes, ensuring that the bounding boxes stay within the decision boundaries of linear predicates (Linear Constraints on Bounding Boxes).

The problem is computationally challenging due to the exponential growth of corner points as d increases. To address scalability, we relax the linear constraints on the bounding boxes by enforcing that only a sampled subset of corners satisfies a subset of the linear constraints. In addition, we

introduce a secondary objective aimed at minimizing the extent (or span) of the bounding boxes along each dimension. Thus, the new objective is formulated as follows:

$$\text{Maximize } \sum_{i=1}^n \sum_{k=1}^m \alpha_{i,k} - \gamma \sum_{k=1}^m \sum_{j=1}^d (x_{\max,k,j} - x_{\min,k,j})$$

where the parameter γ governs the trade-off between maximizing the number of contained points and minimizing the span of the bounding boxes. This relaxation does not significantly degrade the quality of the solution because, on one hand, linear constraints only approximate the true boundaries of the data manifold, and some constraints may be erroneous, allowing for certain violations. On the other hand, minimizing the size of the bounding boxes increases the likelihood that these linear constraints will be satisfied in general.

Finally, a universal guideline for improving interpretability across all three types of explanations is to remove less relevant features. The central idea of such dimensionality reduction is to select features whose exclusion results in minimal loss of accuracy in the extracted rule models. This can be easily implemented in many ways, so we will not elaborate further on this topic.

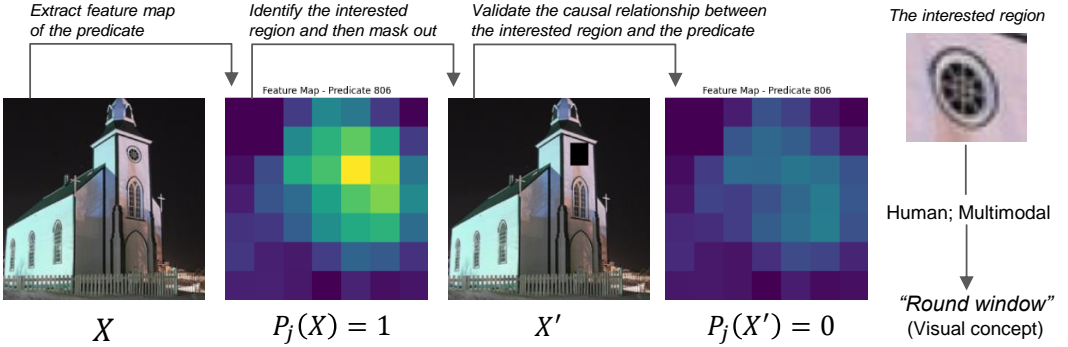


Fig. 3. Grounding deep hidden predicates in high-level visual concepts for interpretability.

Grounding predicates in large, complex neural networks. For large, complex classification neural networks, such as ResNet, which typically use a single fully connected layer as the output layer, NEUROLOGIC operates on this layer to generate a set of rules with deep hidden predicates that cannot be explained as easily as simple linear transformations. In fact, since the inputs undergo a series of complex transformations before being mapped into predicates, backtracking to determine how these predicates specify decision boundaries poses a significant challenge. Even if we can express these decision boundaries using specific rules or formulas in the input space, such complex systems are difficult to comprehend.

However, human cognition typically prefers high-level concepts over low-level features [Chalmers et al. 1992]. For example, when perceiving an image, we focus more on objects than on their edges or corners. Similarly, when reading a sentence, we prioritize individual words rather than individual letters. To address the above challenge, we propose grounding hidden predicates in high-level concepts rather than raw input features. This idea aligns with recent studies on "hidden semantics" [Bau et al. 2019; Voynov and Babenko 2020; Yang et al. 2021]. In this work, we focus on interpreting image classification models, although our method can also be applied to other classification tasks.

Let us consider a set of predicates $\{P_j\}$ obtained following the decoding phase, where $P_j(x) := \mathcal{I}_{z_j^{(L-1)}(x) \geq t_j}$ for the last fully connected layer $L - 1$. For each predicate $P_j(x)$, it is computed through

average pooling over a 7×7 feature map $f_j(x)$, i.e., $z_j^{(L-1)}(x) = \text{average}(f_j(x))$. To proceed, we first interpolate the feature map $f_j(x)$ to match the dimensions of the input image x and subsequently identify the region of interest within the image based on the elevated values in the interpolated feature map. To assess whether this region contributes meaningfully to the computation of predicate $P_j(x)$, we mask out the region of interest and feed the resulting image x' into the model to compute $P_j(x')$. A significant reduction in the activation value $z_j^{(L-1)}(x) - z_j^{(L-1)}(x')$, causing P_j to transition from activation to deactivation, serves as causal evidence validating the importance of the identified region. Throughout this process, we iteratively refine and validate the region of interest to more accurately isolate specific high-level visual elements, such as objects or patterns, that activate P_j . Finally, for a set of input images, we manually examine the regions of interest in each image to identify shared high-level visual concepts across these regions. A figure provides an overview of our approach. Moving forward, we plan to incorporate multimodal vision-language models, such as CLIP [Radford et al. 2021], to enhance the efficiency and scalability of our method.

In summary, NEUROLOGIC operates at the final layer, extracting logical rules with deep hidden predicates grounded in high-level (visual) concepts that are interpretable to humans. This approach overcomes the limitations of earlier methods from the 1990s, which relied on layer-by-layer rule generation and rewriting paradigms that struggled to scale with modern deep learning models [Setiono and Liu 1995, 1997].

4 Case Study: The Iris Dataset

To better illustrate the detailed computations of NEUROLOGIC and demonstrate its ability to unravel black-box models, we present a case study on decoding a fully connected neural network trained on the Iris dataset. This dataset consists of three iris species: "Setosa", "Versicolor", and "Virginica", with a total of 150 samples—50 samples from each species. Each sample is characterized by four features: sepal length, sepal width, petal length, and petal width. We perform an 80/20 train-test split and train a three-layer neural network, with two hidden layers, each containing 12 neurons.

Table 1. Summary of NAPs, class-specific neurons (Ω), and high-contribution neurons (Θ) for the Iris dataset. Only the index j is used to represent $N_{j,l}$, as the layer l is specified.

		"Setosa"	"Versicolor"	"Virginica"
NAPs	Layer 1 activated neurons	{3, 4, 7, 10, 11}	{0, 1, 2, 5}	{0, 1, 2, 5, 6, 8, 9}
	Layer 1 deactivated neurons	{1, 5, 6, 8, 9}	\emptyset	{3, 10, 11}
	Layer 2 activated neurons	{4, 5, 7, 8, 9, 10, 11}	{1, 5, 7}	{1, 3, 6}
	Layer 2 deactivated neurons	{0, 1, 2, 3, 6}	{0, 2, 4}	{0, 2, 4, 8, 9, 10, 11}
Class-specific neurons (layer 2)		{4, 8, 9, 10, 11}	\emptyset	{3, 6}
High-contribution neurons (layer 1)		{3, 4, 10, 11}	\emptyset	{5, 6, 8, 9}

In the distilling phase, we compute the global NAPs for each class using a δ value of 0.95. We let NEUROLOGIC to operate on the second hidden layer, where we compute the class-specific neurons (Ω) for each class. For "Setosa", the class-specific neurons are $\{N_{4,2}, N_{8,2}, N_{9,2}, N_{10,2}, N_{11,2}\}$, for "Virginica", they are $\{N_{3,2}, N_{6,2}\}$, while "Versicolor" does not have class-specific neurons. Next, in the decoding phase, we select the top 3 high-contribution neurons (Θ), from layer 1 that most significantly influence each class-specific neuron. We observe that these high-contribution neurons are frequently shared across class-specific neurons. For instance, the top three contributing neurons for neuron $N_{3,2}$ and neuron $N_{6,2}$ are $\{N_{6,1}, N_{5,1}, N_{8,1}\}$ and $\{N_{6,1}, N_{9,1}, N_{8,1}\}$, respectively. We present the results of these steps in Table 1.

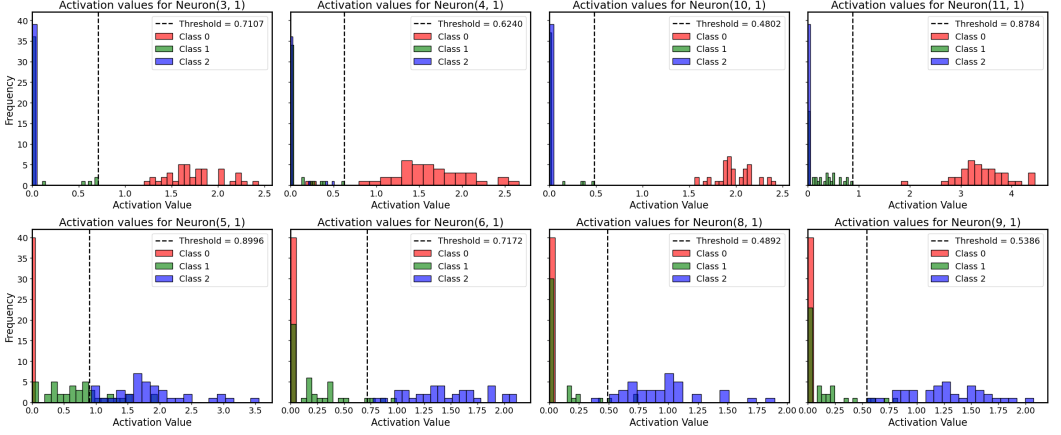


Fig. 4. Activation ranges of high-contribution neurons (Θ) along with their optimal threshold. The first row represents Θ for class "Setosa", while the second row shows those for class "Virginica".

Table 2. The confusion matrix with predicate patterns (conjunctive forms). The first row represents the classes, and the second column lists the patterns for each class. Each entry shows the number of training and test data points that follow the corresponding patterns, reported before and within parentheses, respectively.

		"Setosa"	"Versicolor"	"Virginica"
"Setosa"	$P_3 \wedge P_4 \wedge P_{10} \wedge P_{11}$	39(10)	0(0)	0(0)
	$P_3 \wedge \neg P_4 \wedge P_{10} \wedge P_{11}$	1(0)	0(0)	0(0)
"Versicolor"	$\neg (\bigvee_{j \in \{3,4,5,6,8,9,10,11\}} P_j)$	0(0)	29(5)	0(0)
	$P_5 \wedge \neg (\bigvee_{j \in \{3,4,6,8,9,10,11\}} P_j)$	0(0)	8(2)	0(0)
	$P_5 \wedge P_6 \wedge (\bigvee_{j \in \{3,4,8,9,10,11\}} P_j)$	0(0)	1(0)	0(0)
	$P_9 \wedge \neg (\bigvee_{j \in \{3,4,5,6,8,10,11\}} P_j)$	0(0)	1(1)	0(0)
"Virginica"	$P_5 \wedge P_6 \wedge P_8 \wedge P_9$	0(0)	2(1)	38(9)
	$P_5 \wedge P_6 \wedge \neg P_8 \wedge P_9$	0(0)	0(0)	1(2)

Next, we generate a set of predicates by computing optimal thresholds for the activation range of each high-contribution neuron. We observe that these thresholds effectively help distinguish the corresponding class from others, as illustrated in Figure 4. Then, we feed all the training and test data into these predicates and collect their patterns for each class, as shown in Table 2. By performing some simple merging operations on these predicates to make them more general, we derive the following rules (explaining the network with linear constraints):

$$P_5 \wedge P_6 \wedge P_9 \Rightarrow \text{"Virginica"}; \quad P_3 \wedge P_{10} \wedge P_{11} \Rightarrow \text{"Setosa"}; \quad \neg(P_3 \vee P_4 \vee P_8 \vee P_{10} \vee P_{11}) \Rightarrow \text{"Versicolor"}$$

Despite the absence of specific predicates for "Versicolor", it can be recognized using the predicates of the other two classes, as shown by the third rule above. It is also surprising to see that the confusion matrix of our rule-based model is identical to that of the original neural network. Additionally, it generalizes to test data in exactly the same manner as the original model.

In addition, to achieve better interpretability, we assume that the data follows bounding box priors and search for individual feature-split-based explanations by solving the corresponding MILP problem. For the solver, we use PuLP, a Python library for defining and solving MILP problems. In our solution, $P_3 \wedge P_{10} \wedge P_{11}$ can be refined to a bounding box $[[-1.870, 2.492], [-2.434, 3.091], [-1.568, -0.743], [-1.447, 1.447]]$, which can be simplified to a rule, $\text{Petal.length} \leq -0.743 \Rightarrow \text{"Setosa"}$, as other corner values could

cover the entire training data. Further, we show that the rule for "Virginica" can be grounded in input features through the following rules:

$$(\text{Petal.length} \geq 0.678 \wedge \text{Petal.width} \leq 0.725) \vee (\text{Petal.length} \geq 0.564 \wedge \text{Petal.width} \geq 0.725) \Rightarrow \text{"Virginica"}$$

To compare with the baseline, we generate a decision tree solution, as presented in Figure 5. Notably, the decision tree and our rules share many similarities. For instance, they both use Petal.length as the primary feature to distinguish "Setosa" from the other classes. Our rule-based model also achieve an accuracy of 95.83%, which is comparable to the decision tree's accuracy of 96.67%.

5 Evaluation

In this section, we apply our NEUROLOGIC approach to two challenging instances, evaluating its capability to generate global and interpretable logic rules. We also discuss existing work as a baseline for comparison with our approach.

5.1 Fully Connected Neural Network with the MNIST Benchmark

In the first experiment, unlike the case study in Section 4, we apply NEUROLOGIC to a significantly larger fully connected neural network with a more complex input space. Specifically, we use the mnistfc_256x4 model [VNNCOMP 2021], a 4-layer fully connected network with 256 neurons per layer, pre-trained on the MNIST dataset. The MNIST dataset consists of over 60,000 training samples, each of size 28x28 pixels.

We begin by computing the global NAPs for each class with a δ value of 0.95, followed by applying NEUROLOGIC to the second hidden layer to identify class-specific neurons. Unlike our observations in the case study, we find that each class here has its own distinct set of class-specific neurons, averaging around 9 neurons, though the numbers vary considerably. For example, class 0 has 14 class-specific neurons, while class 8 has only one. Next, we select the top 10 most contributing neurons for each class-specific neuron. Interestingly, we observe that these high-contributing neurons are commonly shared among class-specific neurons, resulting in an average of 18.2 high-contributing neurons for each class. Notably, class 0 has only 17 high-contributing neurons despite having the most class-specific neurons.

We then determine the optimal threshold for each high-contributing neuron to generate a set of predicates. Subsequently, we derive a set of rules for each class by feeding all the training data into these predicates to collect their activation patterns. Due to outliers and wrong instances, we may mistakenly collect "outlier" patterns. Upon close inspection, such patterns exhibit a common characteristic: they have many fewer activated predicates and are exhibited by very few instances. For instance, class 0 has a total of 10 patterns with less than 3 activated predicates each, and only 32 instances follow them. Thus, we remove those conjunctive forms that contain less than 3 activations for each class. After removal, each class has an average of 1636.5 disjunctive forms.

Unlike the decision rule in neural networks, where the highest logit is classified as the output class, for our rule-based models, we classify an instance as belonging to a certain class if it meets the following two conditions simultaneously: 1) it can be explained by that class's rules, i.e., a matched pattern is found; 2) it cannot be explained by the rules of any other classes. If an instance can match patterns from multiple classes, then the model simply reports the matched conditions rather than leaning towards a choice like neural networks do. This is also a much safer practice than

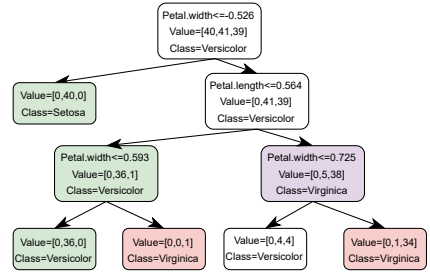


Fig. 5. Decision Tree of Iris Dataset

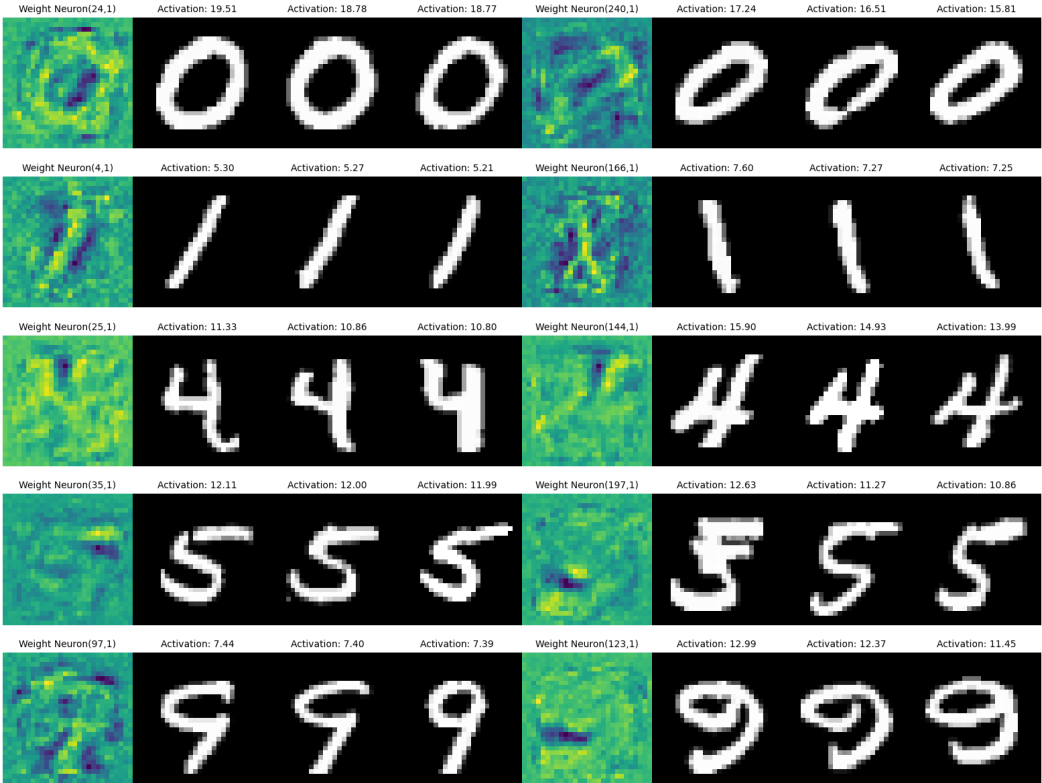


Fig. 6. The hidden predicates capture meaningful patterns corresponding to each digit. The first and fifth columns illustrate the weights associated with selected hidden predicate, reshaped to a 28×28 grid, while the remaining columns display input samples that activate these predicates.

neural networks, as rule-based models only make a decision when they are confident and provide their reasoning process—matched rules—to humans for inspection when a confusing classification case occurs. Surprisingly, we find that our rule-based model can still achieve a high classification accuracy of 91.32%, which is not a significant drop from the original neural network’s accuracy of 99.09%. The rule-based model also generalizes well to unseen data, achieving a test set accuracy of 89.38%, which is only a fraction lower than the original neural network’s accuracy of 97.64%. We searched for comparable baselines but found that most existing work does not scale to our benchmark. The most relevant result on rule extraction is from DeepRED [Zilke et al. 2016], which evaluates on a neural network consisting of only 15 hidden neurons. We attempted to scale it to the `mnistfc_256x4` model, but it consistently aborted. Nonetheless, we report an accuracy of 97.52% on the full training set of 60,000 images, which is comparable to their accuracy of 99.60% on only a subset of 12,056 images in binary classification mode, though this is certainly not a fair comparison.

To further enhance interpretability, we ground hidden predicates in the input space using domain knowledge. In this case, as we know that the inputs are images, we have the following prior knowledge: 1) Higher values indicate greater pixel activation; 2) Pixels in certain locations tend to be strongly correlated; 3) The affine transformation of hidden predicates is essentially a convolution with a filter of size 28×28 . Under this view, we observe that these filters encode global templates of certain digits rather than the local features commonly found in CNNs, as illustrated in Figure

6. It is noteworthy that some predicates tend to attend to different types of the same digit. For example, P_4 and P_{166} , which encode the digit 1, tend to lean toward the left and right, respectively. Some predicates are compositional, encoding different parts of a digit. For instance, P_{35} encodes the upper half of digit 5, while P_{197} encodes the lower half. Regardless of the predicate’s preference, they activate when instances significantly overlap with their filter. Thus, the rule governing the grounding of predicates in the input space can be expressed as:

$$P_j = \text{True if } M(B(x, t_x), B(P_j, t_j)) > \text{threshold, else False,}$$

where $B(\cdot, t)$ binarizes the input using threshold t , $B(x, t_x)$ and $B(P_j, t_j)$ represent the positions of high-value pixels in the input and high-value weights in the predicate, with thresholds t_x and t_j , respectively. $M(\cdot, \cdot)$ counts the number of matches. With some simple tuning of these parameters, the final model, which combines the predicate rule and grounding rule, achieves a decent accuracy of 83.44%. We leave improvements in the model’s performance for future work.

5.2 ResNet with the ImageNet Benchmark

In our second experiment, we apply the NEUROLOGIC framework to the ResNet50 model, which is pre-trained on the ImageNet dataset. In this scenario, NEUROLOGIC operates on the output layer, meaning that the class-specific neurons are essentially its output neurons for each class. We select the top 15 high-contribution neurons for each class-specific neuron, resulting in 15 hidden predicates per class. We do not perform any removal of those conjunctive forms in this case, as all predicate appears quite often across the input samples of the corresponding class. Each class has an average of 236 disjunctive forms. The accuracy of the original model is 76.13%, whereas our extracted rule-based model can achieve a considerable accuracy of 71.27%.

Then, in the grounding phase, we employ the causal inference approach detailed in Section 3.4 to assess whether these hidden predicates indeed capture high-level visual concepts that are intelligible to humans, which constitutes the primary objective of this experiment. Surprisingly, we make many interesting observations, some of which might have been overlooked by existing research in probing the "hidden semantics" of vision models. We discuss a few of them here:

A high-level visual concept can be encoded by multiple predicates. For instance, the predicates P_{1007} and P_{940} both encode the visual concept of "dog nose" for the class "English Springer", as illustrated in the first row of Figure 7, where the first four image samples activate P_{1007} and the last two image samples activate P_{940} . Our observations suggest that P_{1007} primarily focuses on the nose, including the areas around the two nostrils, while P_{940} appears to focus more on the region above the nostrils and below the eyes. Despite these differences in focus, we believe both predicates encode the same visual concept, as it is challenging to precisely define the boundaries of the "nose" area.

A predicate can encode similar high-level visual concepts for different classes. To provide a concrete example, we observe that predicates P_{538} and P_{1196} both encode similar types of visual concepts in the classes "Garbage Truck" and "Church". To be more specific, P_{538} tends to focus on structural elements: in the class "Church", it is activated by objects like the window or door on the main buildings of the church, while in the class "Garbage Truck", it focuses on the windshield or side windows of the truck’s front. Similarly, P_{1196} highlights the environmental context in both classes; for the class "Church", it activates around surrounding features such as the sky, trees, or mountains behind the building, while in the "Garbage Truck" class, it focuses on elements like the road, tree lawn, or buildings along the roadside.

A predicate can attend to multiple objects of the same visual concept across the image. As illustrated in the second and fourth rows of Figure 7, P_{2030} attends to both ears of the dog, whereas P_{1231} attends to multiple tires of the garbage truck. This suggests that these predicates function as global concept detectors, one of the merits of which consists in our extracted rule model.

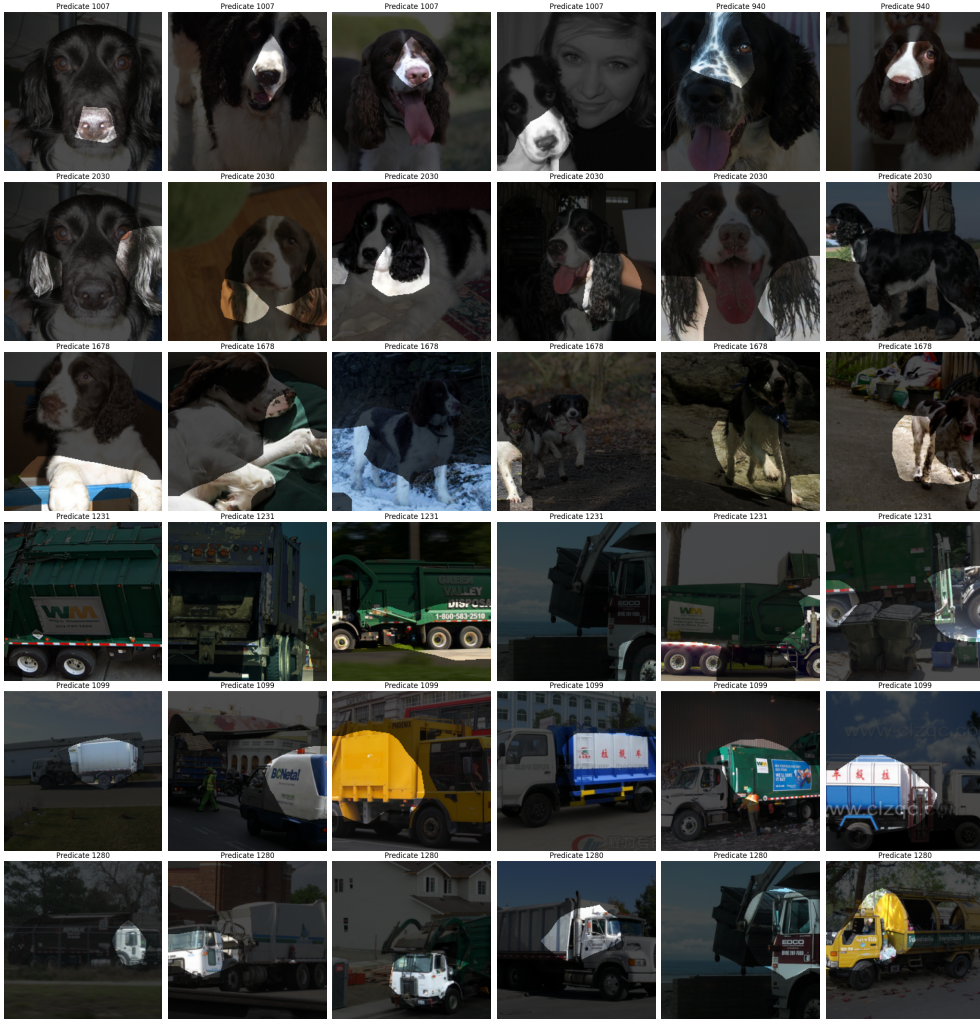


Fig. 7. Hidden predicates grounded in visual concepts. Each row represents a collection of images along with their regions of interest that activate certain predicates. The regions of interest are highlighted, whereas the rest of the image is faded.

A predicate can robustly identify visual concepts despite their varying appearances. The human vision system can recognize objects sharing the same functionality or concepts, regardless of their significant differences in appearance, such as color and shape. Interestingly, we observe that our learned predicates seem to exhibit a similar ability. For example, in the fifth and sixth rows of Figure 7, despite the bodies of the garbage trucks being presented in diverse colors, shapes, and orientations, P_{1196} can robustly attend to them. Similarly, P_{1280} can capture the varying forms and sizes of the garbage truck heads.

To summarize, our learned hidden predicates indeed encode high-level visual concepts that are highly understandable to humans. Along with the logic rules we extracted in the decoding phase, we are able to decode the reasoning process of large and complex CNNs into a set of interpretable

rules. For instance, based only on predicates we introduced in Figure 7, we have the following rules:

$$\begin{aligned} \text{"Nose"} \wedge \text{"Ears"} \wedge \text{"Legs"} &\Rightarrow \text{"English Springer"} \text{ (dog)} \\ \text{"Tires"} \wedge \text{"Truck Body"} \wedge \text{"Truck Head"} &\Rightarrow \text{"Garbage Truck"} \end{aligned}$$

which accurately describe 892/892 and 779/904 samples for the classes "English Springer" and "Garbage Truck" respectively. As for the baseline, our search has not yielded any existing work that generates a rule-based model analogous to ours. Perhaps the most pertinent work in this regard is [Jiang et al. 2024], which identifies rule-like structures, including "disjunctive" and "compositional" behaviors within CNNs. Additionally, other related work [Banerjee et al. 2024; Wong et al. 2021] recognize the significance of the final decision layer. However, these studies concentrate on examining its sparsity and robustness, rather than the derivation of explicit rules.

For future work, we plan to extend our NEUROLOGIC framework to decode more fine-grained rules from deep neural networks, specifically to express the reasoning process of neural networks using rules based on lower-level visual concepts. Ideally, this will help to open the "black box" of the hierarchical reasoning process in DNNs from shallow to deep layers. Additionally, we are considering the use of multimodal models, such as CLIP, to replace human agents in recognizing visual concepts, with the goal of improving efficiency in future work.

6 Related Work

The use of logic rules to interpret neural networks has long been an appealing research direction, with studies in this area dating back to the pre-deep learning era. These approaches can be categorized into two types: local and global methods. Local methods focus on explaining individual predictions by generating rules specific to a single input or a small set of inputs, capturing how the model arrives at a particular decision [Dhurandhar et al. 2018; Goyal et al. 2019; Pedapati et al. 2020; Wachter et al. 2017]. In contrast, global methods offer a comprehensive explanation by deriving a single set of rules that represents the overall behavior of the target model, and are therefore preferred over local methods most of the time, thus will be the main focus of this discussion.

These approaches can be further divided into two groups: pedagogical approaches [Zhang et al. 2021b] and decompositional [Craven and Shavlik 1994]. Pedagogical approaches approximate the network in an end-to-end fashion; more specifically, they treat the network as a black box and train classic rule-learning algorithms such as decision tree on samples generated by the network. For instance, classic decision tree learning algorithms like CART [Breiman et al. 1984] and C4.5 [Quinlan 1993] are adopted for decision tree extraction from neural networks [Boz 2002; Craven and Shavlik 1995; Krishnan et al. 1999]. There are also some attempts at extracting fuzzy logic from trained neural networks [Benítez et al. 1997a,b; Castro et al. 2002].

Decompositional approaches utilize network-specific information, such as network structure and learned weights, to extract rules by examining the connections within the network. The central challenge in rule extraction is to find combinations of specific attribute values (or ranges) that maximize the likelihood of accurate predictions [Towell and Shavlik 1993]. This task is manageable only in very small networks; scalability quickly becomes an issue, as the search space grows exponentially with the number of attributes and their possible values. Thus, most existing work aims to propose efficient search strategies. The KT algorithm [Fu 1991] is one of the earliest methods for rule extraction from neural networks. It starts by categorizing input attributes into positive and negative groups based on the signs of their weights. The algorithm identifies combinations of positive attributes that yield a true prediction and then examines negative attributes. For each combination of positive attributes, it searches for negative attributes that can be excluded while maintaining a true output. The extracted rule is formed from this combination for the desired output class. To apply this approach to multi-layer networks, it generates rules layer by layer

and rewrites them to exclude hidden neurons. Towell and Shavlik [1993] introduce the “ M -of- N ” rule style, which can be expressed as follows: If M of these N expressions are true, then Q . Their algorithm is distinguished by two primary features. First, it implements link (weight) clustering, wherein average weights are reassigned within each cluster. Second, it simplifies the network by eliminating unimportant clusters and re-training. Due to its unique rule structure, the M -of- N method significantly reduces the exponential complexity of subset searching algorithms to approximately cubic complexity. NeuroRule [Setiono and Liu 1995] proposes a three-step methodology for rule extraction: (1) training the network and performing pruning, (2) discretizing and clustering the activation values of hidden neurons, and (3) extracting rules layer by layer, followed by rewriting them in a manner similar to previous approaches. NeuroLinear [Setiono and Liu 1997] made a slight modification to the NeuroRule technique, enabling the use of continuous inputs in neural networks. CRED [Sato and Tsukimoto 2001] also explores rule extraction by employing decision trees to generate rule sets that map input features. Recent work [Zarlenga et al. 2021; Zilke et al. 2016] enhances this approach by integrating advances in decision tree algorithms. However, most existing methods cannot scale to large models and are limited by the model’s architecture, typically FCNs. This motivates us to develop a framework like NEUROLOGIC that can decode global and interpretable rules from large, complex deep learning models.

7 Conclusion

In this paper, we introduce NEUROLOGIC, a novel approach for decoding interpretable logic rules from neural networks. NEUROLOGIC first distills the critical reasoning processes of neural networks through neural activation patterns. It then identifies and transforms the important neurons involved in the models’ reasoning processes into hidden predicates. Subsequently, it generates a set of logic rules based on these hidden predicates in a data-driven manner. Unlike many rule-as-explanation approaches proposed before the era of deep learning, NEUROLOGIC can be adapted to a wide range of deep neural networks thanks to its flexible design in the grounding phase. To be more specific, for fully connected neural networks, hidden predicates can be grounded in patterns of original input features under three types of explanations: linear constraints, domain knowledge, and bounding boxes (decision-tree-like explanations). For large, complex vision neural networks, we show how predicates can be grounded in human-understandable visual concepts via causal inference. Our empirical study demonstrates that NEUROLOGIC can extract global and interpretable rules from state-of-the-art models such as ResNet, a task at which existing work struggles. For instance, we extract a logical rule showing that ResNet classifies an image as a dog based on the presence of visual parts such as the “nose”, “legs”, and “ears”. To the best of our knowledge, this is the first time a complex convolutional neural network has been interpreted through explicit logical rules, represented by human-understandable visual concepts. We believe that NEUROLOGIC can help pave the way toward understanding the black-box nature of neural networks.

References

- Pierre Baldi, Peter Sadowski, and Daniel Whiteson. 2014. Searching for exotic particles in high-energy physics with deep learning. *Nature communications* 5, 1 (2014), 4308.
- Debangshu Banerjee, Avaljot Singh, and Gagandeep Singh. 2024. Interpreting Robustness Proofs of Deep Neural Networks. In *The Twelfth International Conference on Learning Representations, ICLR 2024, Vienna, Austria, May 7-11, 2024*. OpenReview.net. <https://openreview.net/forum?id=Ev10F9TWML>
- David Bau, Bolei Zhou, Aditya Khosla, Aude Oliva, and Antonio Torralba. 2017. Network Dissection: Quantifying Interpretability of Deep Visual Representations. In *2017 IEEE Conference on Computer Vision and Pattern Recognition, CVPR 2017, Honolulu, HI, USA, July 21-26, 2017*. IEEE Computer Society, 3319–3327. <https://doi.org/10.1109/CVPR.2017.354>
- David Bau, Jun-Yan Zhu, Hendrik Strobelt, Bolei Zhou, Joshua B. Tenenbaum, William T. Freeman, and Antonio Torralba. 2019. GAN Dissection: Visualizing and Understanding Generative Adversarial Networks. In *7th International Conference on Learning Representations, ICLR 2019, New Orleans, LA, USA, May 6-9, 2019*. OpenReview.net. https://openreview.net/forum?id=Hyg_X2C5FX
- Yoshua Bengio, Aaron Courville, and Pascal Vincent. 2013. Representation learning: A review and new perspectives. *IEEE transactions on pattern analysis and machine intelligence* 35, 8 (2013), 1798–1828.
- José Manuel Benítez, Juan Luis Castro, and Ignacio Requena. 1997a. Are artificial neural networks black boxes? *IEEE Trans. Neural Networks* 8, 5 (1997), 1156–1164. <https://doi.org/10.1109/72.623216>
- José Manuel Benítez, Juan Luis Castro, and Ignacio Requena. 1997b. Are artificial neural networks black boxes? *IEEE Trans. Neural Networks* 8, 5 (1997), 1156–1164. <https://doi.org/10.1109/72.623216>
- Olcay Boz. 2002. Extracting decision trees from trained neural networks. In *Proceedings of the Eighth ACM SIGKDD International Conference on Knowledge Discovery and Data Mining, July 23-26, 2002, Edmonton, Alberta, Canada*. ACM, 456–461. <https://doi.org/10.1145/775047.775113>
- Leo Breiman, J. H. Friedman, Richard A. Olshen, and C. J. Stone. 1984. *Classification and Regression Trees*. Wadsworth.
- Juan Luis Castro, Carlos Javier Mantas, and José Manuel Benítez. 2002. Interpretation of artificial neural networks by means of fuzzy rules. *IEEE Trans. Neural Networks* 13, 1 (2002), 101–116. <https://doi.org/10.1109/72.977279>
- David J Chalmers, Robert M French, and Douglas R Hofstadter. 1992. High-level perception, representation, and analogy: A critique of artificial intelligence methodology. *Journal of Experimental & Theoretical Artificial Intelligence* 4, 3 (1992), 185–211.
- Mark W. Craven and Jude W. Shavlik. 1994. Using Sampling and Queries to Extract Rules from Trained Neural Networks. In *Machine Learning, Proceedings of the Eleventh International Conference, Rutgers University, New Brunswick, NJ, USA, July 10-13, 1994*, William W. Cohen and Haym Hirsh (Eds.). Morgan Kaufmann, 37–45. <https://doi.org/10.1016/B978-1-55860-335-6.50013-1>
- Mark W. Craven and Jude W. Shavlik. 1995. Extracting Tree-Structured Representations of Trained Networks. In *Advances in Neural Information Processing Systems 8, NIPS, Denver, CO, USA, November 27-30, 1995*, David S. Touretzky, Michael Mozer, and Michael E. Hasselmo (Eds.). MIT Press, 24–30. <http://papers.nips.cc/paper/1152-extracting-tree-structured-representations-of-trained-networks>
- Amit Dhurandhar, Pin-Yu Chen, Ronny Luss, Chun-Chen Tu, Pai-Shun Ting, Karthikeyan Shanmugam, and Payel Das. 2018. Explanations based on the Missing: Towards Contrastive Explanations with Pertinent Negatives. In *Advances in Neural Information Processing Systems 31: Annual Conference on Neural Information Processing Systems 2018, NeurIPS 2018, December 3-8, 2018, Montréal, Canada*, Samy Bengio, Hanna M. Wallach, Hugo Larochelle, Kristen Grauman, Nicolò Cesa-Bianchi, and Roman Garnett (Eds.), 590–601. <https://proceedings.neurips.cc/paper/2018/hash/c5ff2543b53f4cc0ad3819a36752467b-Abstract.html>
- Finale Doshi-Velez and Been Kim. 2017. Towards A Rigorous Science of Interpretable Machine Learning. *arXiv: Machine Learning* (2017). <https://api.semanticscholar.org/CorpusID:11319376>
- LiMin Fu. 1991. Rule Learning by Searching on Adapted Nets. In *Proceedings of the 9th National Conference on Artificial Intelligence, Anaheim, CA, USA, July 14-19, 1991, Volume 2*, Thomas L. Dean and Kathleen R. McKeown (Eds.). AAAI Press / The MIT Press, 590–595. <http://www.aaai.org/Library/AAAI/1991/aaai91-092.php>
- Erik Gawehn, Jan A. Hiss, and Gisbert Schneider. 2016. Deep Learning in Drug Discovery. *Molecular Informatics* 35, 1 (2016), 3–14. <https://doi.org/10.1002/minf.201501008> arXiv:<https://onlinelibrary.wiley.com/doi/pdf/10.1002/minf.201501008>
- Chuqin Geng, Nham Le, Xiaojie Xu, Zhaoyue Wang, Arie Gurfinkel, and Xujie Si. 2023. Towards Reliable Neural Specifications. In *International Conference on Machine Learning, ICML 2023, 23-29 July 2023, Honolulu, Hawaii, USA (Proceedings of Machine Learning Research, Vol. 202)*, Andreas Krause, Emma Brunskill, Kyunghyun Cho, Barbara Engelhardt, Sivan Sabato, and Jonathan Scarlett (Eds.). PMLR, 11196–11212. <https://proceedings.mlr.press/v202/geng23a.html>
- Chuqin Geng, Zhaoyue Wang, Haolin Ye, Saifei Liao, and Xujie Si. 2024. Learning Minimal NAP Specifications for Neural Network Verification. *arXiv preprint arXiv:2404.04662* (2024).
- Chuqin Geng, Xiaojie Xu, Haolin Ye, and Xujie Si. 2022. Scalar Invariant Networks with Zero Bias. *CoRR abs/2211.08486* (2022). <https://doi.org/10.48550/ARXIV.2211.08486> arXiv:[2211.08486](https://arxiv.org/abs/2211.08486)

- Athanasios Glentis Georgoulakis, George Retsinas, and Petros Maragos. 2023. Feather: An Elegant Solution to Effective DNN Sparsification. In *34th British Machine Vision Conference 2023, BMVC 2023, Aberdeen, UK, November 20-24, 2023*. BMVA Press, 832–836. <http://proceedings.bmvc2023.org/832/>
- Yash Goyal, Ziyang Wu, Jan Ernst, Dhruv Batra, Devi Parikh, and Stefan Lee. 2019. Counterfactual Visual Explanations. In *Proceedings of the 36th International Conference on Machine Learning, ICML 2019, 9-15 June 2019, Long Beach, California, USA (Proceedings of Machine Learning Research, Vol. 97)*, Kamalika Chaudhuri and Ruslan Salakhutdinov (Eds.). PMLR, 2376–2384. <http://proceedings.mlr.press/v97/goyal19a.html>
- Riccardo Guidotti, Anna Monreale, Franco Turini, Dino Pedreschi, and Fosca Giannotti. 2018. A Survey Of Methods For Explaining Black Box Models. *CoRR* abs/1802.01933 (2018). arXiv:1802.01933 <http://arxiv.org/abs/1802.01933>
- Boris Hanin and David Rolnick. 2019a. Complexity of Linear Regions in Deep Networks. In *ICML (Proceedings of Machine Learning Research, Vol. 97)*. PMLR, 2596–2604.
- Boris Hanin and David Rolnick. 2019b. Deep ReLU Networks Have Surprisingly Few Activation Patterns. In *NeurIPS*. 359–368.
- Kaiming He, Xiangyu Zhang, Shaoqing Ren, and Jian Sun. 2016. Deep Residual Learning for Image Recognition. In *2016 IEEE Conference on Computer Vision and Pattern Recognition, CVPR 2016, Las Vegas, NV, USA, June 27-30, 2016*. IEEE Computer Society, 770–778. <https://doi.org/10.1109/CVPR.2016.90>
- Geoffrey Hinton, Li Deng, Dong Yu, George E. Dahl, Abdel-rahman Mohamed, Navdeep Jaitly, Andrew Senior, Vincent Vanhoucke, Patrick Nguyen, Tara N. Sainath, and Brian Kingsbury. 2012. Deep Neural Networks for Acoustic Modeling in Speech Recognition: The Shared Views of Four Research Groups. *IEEE Signal Processing Magazine* 29, 6 (2012), 82–97. <https://doi.org/10.1109/MSP.2012.2205597>
- Jake M Hofman, Amit Sharma, and Duncan J Watts. 2017. Prediction and explanation in social systems. *Science* 355, 6324 (2017), 486–488.
- Mingqi Jiang, Saeed Khorram, and Li Fuxin. 2024. Comparing the Decision-Making Mechanisms by Transformers and CNNs via Explanation Methods. In *Proceedings of the IEEE/CVF Conference on Computer Vision and Pattern Recognition*. 9546–9555.
- R. Krishnan, G. Sivakumar, and P. Bhattacharya. 1999. Extracting decision trees from trained neural networks. *Pattern Recognit.* 32, 12 (1999), 1999–2009. [https://doi.org/10.1016/S0031-3203\(98\)00181-2](https://doi.org/10.1016/S0031-3203(98)00181-2)
- Alex Krizhevsky, Ilya Sutskever, and Geoffrey E. Hinton. 2012. ImageNet Classification with Deep Convolutional Neural Networks. In *Advances in Neural Information Processing Systems 25: 26th Annual Conference on Neural Information Processing Systems 2012. Proceedings of a meeting held December 3-6, 2012, Lake Tahoe, Nevada, United States*, Peter L. Bartlett, Fernando C. N. Pereira, Christopher J. C. Burges, Léon Bottou, and Kilian Q. Weinberger (Eds.). 1106–1114. <https://proceedings.neurips.cc/paper/2012/hash/c399862d3b9d6b76c8436e924a68c45b-Abstract.html>
- Tailin Liang, John Glossner, Lei Wang, Shaobo Shi, and Xiaotong Zhang. 2021. Pruning and quantization for deep neural network acceleration: A survey. *Neurocomputing* 461 (2021), 370–403.
- Zachary Chase Lipton. 2016. The Mythos of Model Interpretability. *CoRR* abs/1606.03490 (2016). arXiv:1606.03490 <http://arxiv.org/abs/1606.03490>
- Yongjin Park and Manolis Kellis. 2015. Deep learning for regulatory genomics. *Nature biotechnology* 33, 8 (2015), 825–826.
- David Parks, J Xavier Prochaska, Shawfeng Dong, and Zheng Cai. 2018. Deep learning of quasar spectra to discover and characterize damped Ly systems. *Monthly Notices of the Royal Astronomical Society* 476, 1 (01 2018), 1151–1168. <https://doi.org/10.1093/mnras/sty196> arXiv:<https://academic.oup.com/mnras/article-pdf/476/1/1151/24261051/sty196.pdf>
- Tejaswini Pedapati, Avinash Balakrishnan, Karthikeyan Shanmugam, and Amit Dhurandhar. 2020. Learning Global Transparent Models consistent with Local Contrastive Explanations. In *Advances in Neural Information Processing Systems 33: Annual Conference on Neural Information Processing Systems 2020, NeurIPS 2020, December 6-12, 2020, virtual*, Hugo Larochelle, Marc'Aurelio Ranzato, Raia Hadsell, Maria-Florina Balcan, and Hsuan-Tien Lin (Eds.). <https://proceedings.neurips.cc/paper/2020/hash/24aef8cb3281a2422a59b51659f1ad2e-Abstract.html>
- Dino Pedreschi, Fosca Giannotti, Riccardo Guidotti, Anna Monreale, Salvatore Ruggieri, and Franco Turini. 2019. Meaningful Explanations of Black Box AI Decision Systems. In *The Thirty-Third AAAI Conference on Artificial Intelligence, AAAI 2019, The Thirty-First Innovative Applications of Artificial Intelligence Conference, IAAI 2019, The Ninth AAAI Symposium on Educational Advances in Artificial Intelligence, EAAI 2019, Honolulu, Hawaii, USA, January 27 - February 1, 2019*. AAAI Press, 9780–9784. <https://doi.org/10.1609/AAAI.V33I01.33019780>
- J. Ross Quinlan. 1993. *C4.5: Programs for Machine Learning*. Morgan Kaufmann.
- Alec Radford, Jong Wook Kim, Chris Hallacy, Aditya Ramesh, Gabriel Goh, Sandhini Agarwal, Girish Sastry, Amanda Askell, Pamela Mishkin, Jack Clark, et al. 2021. Learning transferable visual models from natural language supervision. In *International conference on machine learning*. PMLR, 8748–8763.
- Makoto Sato and Hiroshi Tsukimoto. 2001. Rule extraction from neural networks via decision tree induction. In *IJCNN'01. International Joint Conference on Neural Networks. Proceedings (Cat. No. 01CH37222)*, Vol. 3. IEEE, 1870–1875.

- Ramprasaath R. Selvaraju, Abhishek Das, Ramakrishna Vedantam, Michael Cogswell, Devi Parikh, and Dhruv Batra. 2017. Grad-CAM: Visual Explanations from Deep Networks via Gradient-Based Localization. In *2017 IEEE International Conference on Computer Vision (ICCV)*. 618–626. <https://doi.org/10.1109/ICCV.2017.74>
- Rudy Setiono and Huan Liu. 1995. Understanding Neural Networks via Rule Extraction. In *Proceedings of the Fourteenth International Joint Conference on Artificial Intelligence, IJCAI 95, Montréal Québec, Canada, August 20-25 1995, 2 Volumes*. Morgan Kaufmann, 480–487. <http://ijcai.org/Proceedings/95-1/Papers/063.pdf>
- Rudy Setiono and Huan Liu. 1997. NeuroLinear: From neural networks to oblique decision rules. *Neurocomputing* 17, 1 (1997), 1–24. [https://doi.org/10.1016/S0925-2312\(97\)00038-6](https://doi.org/10.1016/S0925-2312(97)00038-6)
- David Silver, Julian Schrittwieser, Karen Simonyan, Ioannis Antonoglou, Aja Huang, Arthur Guez, Thomas Hubert, Lucas Baker, Matthew Lai, Adrian Bolton, Yutian Chen, Timothy P. Lillicrap, Fan Hui, Laurent Sifre, George van den Driessche, Thore Graepel, and Demis Hassabis. 2017. Mastering the game of Go without human knowledge. *Nat.* 550, 7676 (2017), 354–359. <https://doi.org/10.1038/NATURE24270>
- Ilya Sutskever, Oriol Vinyals, and Quoc V. Le. 2014. Sequence to Sequence Learning with Neural Networks. In *Advances in Neural Information Processing Systems 27: Annual Conference on Neural Information Processing Systems 2014, December 8-13 2014, Montreal, Quebec, Canada*, Zoubin Ghahramani, Max Welling, Corinna Cortes, Neil D. Lawrence, and Kilian Q. Weinberger (Eds.). 3104–3112. <https://proceedings.neurips.cc/paper/2014/hash/a14ac55a4f27472c5d894ec1c3c743d2-Abstract.html>
- Christian Szegedy, Wojciech Zaremba, Ilya Sutskever, Joan Bruna, Dumitru Erhan, Ian J. Goodfellow, and Rob Fergus. 2014. Intriguing properties of neural networks. In *2nd International Conference on Learning Representations, ICLR 2014, Banff, AB, Canada, April 14-16, 2014, Conference Track Proceedings*, Yoshua Bengio and Yann LeCun (Eds.). <http://arxiv.org/abs/1312.6199>
- Geoffrey G. Towell and Jude W. Shavlik. 1993. Extracting Refined Rules from Knowledge-Based Neural Networks. *Mach. Learn.* 13 (1993), 71–101. <https://doi.org/10.1007/BF00993103>
- VNNCOMP. 2021. VNNCOMP. <https://sites.google.com/view/vnn2021>
- Andrey Voynov and Artem Babenko. 2020. Unsupervised Discovery of Interpretable Directions in the GAN Latent Space. In *Proceedings of the 37th International Conference on Machine Learning, ICML 2020, 13-18 July 2020, Virtual Event (Proceedings of Machine Learning Research, Vol. 119)*. PMLR, 9786–9796. <http://proceedings.mlr.press/v119/voynov20a.html>
- Sandra Wachter, Brent D. Mittelstadt, and Chris Russell. 2017. Counterfactual Explanations without Opening the Black Box: Automated Decisions and the GDPR. *CoRR* abs/1711.00399 (2017). arXiv:1711.00399 <http://arxiv.org/abs/1711.00399>
- Tong Wang. 2019. Gaining Free or Low-Cost Interpretability with Interpretable Partial Substitute. In *Proceedings of the 36th International Conference on Machine Learning, ICML 2019, 9-15 June 2019, Long Beach, California, USA (Proceedings of Machine Learning Research, Vol. 97)*, Kamalika Chaudhuri and Ruslan Salakhutdinov (Eds.). PMLR, 6505–6514. <http://proceedings.mlr.press/v97/wang19a.html>
- Eric Wong, Shibani Santurkar, and Aleksander Madry. 2021. Leveraging Sparse Linear Layers for Debuggable Deep Networks. In *Proceedings of the 38th International Conference on Machine Learning, ICML 2021, 18-24 July 2021, Virtual Event (Proceedings of Machine Learning Research, Vol. 139)*, Marina Meila and Tong Zhang (Eds.). PMLR, 11205–11216. <http://proceedings.mlr.press/v139/wong21b.html>
- Mike Wu, Sonali Parbhoo, Michael C. Hughes, Ryan Kindle, Leo A. Celi, Maurizio Zazzi, Volker Roth, and Finale Doshi-Velez. 2020. Regional Tree Regularization for Interpretability in Deep Neural Networks. In *The Thirty-Fourth AAAI Conference on Artificial Intelligence, AAAI 2020, The Thirty-Second Innovative Applications of Artificial Intelligence Conference, IAAI 2020, The Tenth AAAI Symposium on Educational Advances in Artificial Intelligence, EAAI 2020, New York, NY, USA, February 7-12, 2020*. AAAI Press, 6413–6421. <https://doi.org/10.1609/AAAI.V34I04.6112>
- Ceyuan Yang, Yujun Shen, and Bolei Zhou. 2021. Semantic Hierarchy Emerges in Deep Generative Representations for Scene Synthesis. *Int. J. Comput. Vis.* 129, 5 (2021), 1451–1466. <https://doi.org/10.1007/S11263-020-01429-5>
- Mateo Espinosa Zarlenga, Zohreh Shams, and Mateja Jamnik. 2021. Efficient compositional rule extraction for deep neural networks. *arXiv preprint arXiv:2111.12628* (2021).
- Yu Zhang, Peter Tiño, Ales Leonardis, and Ke Tang. 2021a. A Survey on Neural Network Interpretability. *IEEE Trans. Emerg. Top. Comput. Intell.* 5, 5 (2021), 726–742. <https://doi.org/10.1109/TETCI.2021.3100641>
- Yu Zhang, Peter Tiño, Ales Leonardis, and Ke Tang. 2021b. A Survey on Neural Network Interpretability. *IEEE Trans. Emerg. Top. Comput. Intell.* 5, 5 (2021), 726–742. <https://doi.org/10.1109/TETCI.2021.3100641>
- Wayne Xin Zhao, Kun Zhou, Junyi Li, Tianyi Tang, Xiaolei Wang, Yupeng Hou, Yingqian Min, Beichen Zhang, Junjie Zhang, Zican Dong, et al. 2023. A survey of large language models. *arXiv preprint arXiv:2303.18223* (2023).
- Jan Ruben Zilke, Eneldo Loza Mencía, and Frederik Janssen. 2016. Deepred—rule extraction from deep neural networks. In *Discovery Science: 19th International Conference, DS 2016, Bari, Italy, October 19–21, 2016, Proceedings 19*. Springer, 457–473.